JBMR Plus, 2025, **9**, ziaf047
https://doi.org/10.1093/jbmrpl/ziaf047
Advance access publication: April 24, 2025
Methods and Techniques

Monocytes/macrophages contamination disrupts functional and transcriptional characteristics of murine bone marrow- and bone-derived stromal cells

Yuko Kawano[1,2], Hiroki Kawano[1,3], Stephanie Busch[1,2], Allison J. Li[1,2], Jane Zhang[1,2], Noah A. Salama[1,2], Emily R. Quarato[1,2], Mary Georger[1,2], Nataliia Vdovichenko[1,2], Mitra Azadniv[1,3], Daniel K. Byun[1,2,3], Elizabeth A. LaMere[1,2,3], Mark W. LaMere[1,2,3], Jane L. Liesveld[1,3], Michael W. Becker[1,3], Laura M. Calvi[1,2,*]

[1]James P. Wilmot Cancer Institute, University of Rochester School of Medicine and Dentistry, Rochester, NY 14642, United States
[2]Division of Endocrinology and Metabolism, Department of Medicine, University of Rochester School of Medicine and Dentistry, Rochester, NY 14642, United States
[3]Division of Hematology/Oncology, Department of Medicine, University of Rochester School of Medicine and Dentistry, Rochester, NY 14642, United States

*Corresponding author: Laura M. Calvi, Division of Endocrinology and Metabolism, Department of Medicine, University of Rochester School of Medicine, 601 Elmwood Ave, Box 693, Rochester, NY 14642, United States (laura_calvi@urmc.rochester.edu)

Abstract

Stromal cells are critical regulators of hematopoietic stem/progenitor cells and skeletal homeostasis. Although precise systems for functional analysis are critical to investigate mechanistically bone and bone marrow (BM)-derived stromal cells, the establishment of reproducible, highly enriched ex vivo methods for stromal cell isolation, culture and evaluation have been challenging, leading to inconsistent data on stromal cell function. In this work, we carefully tested ex vivo culture of murine stromal cells from BM and bone and discovered abundant and persistent contamination of monocytes and macrophages. We succeeded in establishing highly enriched ex vivo culture system for stromal cells by eliminating persistent monocytes and macrophages using selection against the immunological markers F4/80, Ly6C, and CD45. Transcriptional and functional assays of enriched stromal cell culture revealed differential characteristics of stromal cells from different origins, a dormant signature for bone-derived cells and a highly proliferative progenitor-like signature for BM-derived cells. Monocyte and macrophage contamination reduced signatures of immature stromal cells such as expression levels of SOX9 and CD140a as well as the cells' ability to support hematopoietic stem and progenitor cells based on our growth factor-free co-culture system of hematopoietic cells and stromal cells followed by in vivo functional assays. The inhibitory effects of macrophages on stromal cells may be explained by their potent production of inflammatory cytokines such as CXCL2, CCL3, and complement factor (C1q) confirmed by protein immunoassay of culture supernatant, as well as the differential contribution of pre-osteoblasts to the stromal cell population. This study highlights the functional diversity of stromal cells depending on the microenvironment of origin while addressing a critical limitation of murine ex vivo systems. Our robust culture system enables the study of isolated stromal cells function as well as the impact of stromal cells-macrophage crosstalk.

Keywords: stromal cells, monocyte/macrophage, macrophage-stromal cell crosstalk, supporting effect of hematopoietic cells, ex vivo co-culture system

Lay Summary

Bone and bone marrow (BM) derived stromal cells support skeletal and hematopoietic homeostasis, growth and response to injury, aging, and disease. However, purifying these cells to investigate their functions presents technical difficulties including evaluation of purity and establishment of highly enriched culture ex vivo. We identified persistent contamination of macrophages and their precursors, monocytes, which are innate immune cell populations critical for homeostasis as well as response to tissue injury. We found that this monocyte/macrophage contamination in bone and BM isolation of stromal cells fundamentally changed the function of the stromal cells, since complete removal uncovered different abilities to differentiate and to support blood stem cells. We also found through this novel isolation and culture system that the true signature of stromal cells depends on the compartment of the skeleton (bone or marrow) from which they are derived. These findings provide a powerful tool to investigate more accurately the function of stromal cells and show that monocytes/macrophages have profound impact on stromal cells.

Received: May 1, 2024. **Revised:** February 17, 2025. **Accepted:** March 11, 2025

Introduction

Stromal cells, formerly known as mesenchymal stromal cells, are a heterogeneous population of non-blood forming skeletal cells in the bone marrow microenvironment (BMME). These cells include stem and progenitor cells with self-renewal and multi-lineage differentiation potential toward the osteoblastic, chondrocytic and adipocytic cell lineages.[1,2] Murine stromal cells have been characterized by their cell surface marker expression, genetic lineage marking studies, and single cell transcriptomic analysis.[1,3] We and others identify stromal cells by the negative expression of CD45 (general hematopoietic marker), B220/CD3e/Ter119 (B cell, T cell, and erythroid: Lineage marker: Lin), and CD31 (endothelial cell marker),[1,3,4] with positive expression of CD51 (extracellular Nestin$^+$ stromal cell marker)[5] and variable expression of Sca1 (stem cell antigen-1).[6–8] Stromal cells have increasingly gained attention as important regulators of skeletal and hematopoietic homeostasis, where stromal cells play an important role in supporting hematopoietic stem cells (HSCs).[1,3,7,9,10] However, current protocols to isolate stromal cells from bone marrow (BM) typically involve washing off the non-adherent hematopoietic cells and assuming the adherent population that remains represents the stromal population.[11,12] While this method is effective for human BM samples,[13] we and others[14] have found that significant contamination of macrophages still remains in the adherent population of murine whole BM and bone associated cell cultures. This contaminating population would be expected to confound functional and mechanistic analysis of stromal cells and to interfere with experimental outcomes. In this study, we carefully tested conventional protocols for purity, devised novel methods to ensure purity of stromal cells, and studied phenotypic, transcriptional, and functional consequences of macrophages contamination in BM and bone derived stromal cells. We found that removal of monocytes, macrophages and their progenitors was critical to successfully isolating and expanding stromal cells from BM and bone. Moreover, once purified, distinct stromal cell populations were identified from BM compared to those isolated from bone. Importantly, monocyte and macrophage contamination in vitro impacts stromal cell function, potentially via cell–cell interaction and production of inflammatory factors. Therefore, it is crucial to adopt techniques to achieve highly purified mouse stromal cells from ex vivo culture for functional studies of the transcriptome, secretome, or regulatory properties of stromal cells.

Materials and methods

Mice

Mice were obtained from Jackson Laboratory and maintained in the Vivarium facility at the University of Rochester School of Medicine and Dentistry in accordance with protocols approved by the Institutional Animal Care and Use Committee. All strains were of the C57BL/6 background and express the Ly5.2 allotype of CD45 (CD45.2) unless noted otherwise. Strains used include C57BL/6J and Sox9-GFP mice which were genotyped by PCR using primer sequences publicly available through the Jackson Laboratory. This study was performed in accordance with ARRIVE guidelines.[15]

Flow cytometry

Analysis of marrow cell populations was performed as previously described.[7] For marrow cell analysis, marrow was released by crushing with a mortar and pestle in PBS. For BM analysis for stromal cell populations, BM cells were digested in 2 mL HBSS (Gibco, Thermo Fisher Scientific, #14175-095) containing 1 mg/mL Collagenase type IV (Sigma-Aldrich, #C5138), and 2 mg/mL dispase (Gibco, #17105-041) for 30 min in 37 °C water bath. Digested BM cells were collected and washed with 3 mL of FACS buffer 2% FBS/PBS) for the analysis. For stromal cell analysis for bone-associated cells, murine hind limbs and pelvis were digested as described in bone-derived stromal cell (BSC) culture section. Samples were run on a BD LSR Fortessa flow cytometer: 5 lasers, UV (355 nm), violet (405 nm), blue (488 nm), yellow-green (561 nm), and red (640 nm) (BD Biosciences). As a dead stain, DAPI was used. Analysis was performed using FCS Express version 7 (De Novo Software). The gating strategy used to identify populations enriched for cells of interest has been described in the main text. Sorting was performed on a FACSAriaII with 405-, 488-, 532-, and 640-lasers (BD Biosciences) at the University of Rochester Medical Center Flow Core. The information of antibodies utilized for flow cytometry is provided in Table S1.

Plate coating with rat collagen type I

The tissue treated culture plates were coated with collagen Type I (rat tail) (Corning, #354236) according to the manufacturer's protocol. Briefly, 50 μg/mL of Collagen Type I solution was prepared using 0.02 N acetic acid and then dispensed as 5 $\mu g/cm^2$ in the designated plates followed by overnight incubation at room temperature. On the following day, the plates were washed with PBS once and stored at 4 °C. Collagen solution was reused once.

BM-derived stromal cells culture

Cells were isolated from crushed hind limbs and pelvic bones of male C57BL/6 mice and dissociated in FACS buffer (PBS with 2% heat inactivated fetal bovine serum (FBS, Gemini Bio-Products) using 18G needles. Cells were then plated whole at a density of 2.2×10^5 cells/cm^2 in αMEM without ascorbic acid (Gibco, #A1049001) with 10% FBS and 1x penicillin/streptomycin (P/S) (Gibco, #15140-122), or according to treatment conditions described below. For the improved protocol, we flushed BM cells from a pair of tibias, femurs, and humeri directly onto a Collagen Type I-precoated 10 cm dish (Corning #430293) containing αMEM (without ascorbic acid) with 15% FBS and 1x P/S. After gently swirling the dishes, cells were placed in a hypoxia incubator (2% O_2, 5% CO_2 at 37 °C). The first media change was done on day 5, and cells were sorted on the following day as described below.

Bone-derived stromal cell culture

Bone pieces from crushed hind limb and pelvic bones of male C57BL/6 mice were washed out of BM cells and digested for 30 min in 1 mL of collagenase type I (Stemcell Technologies, # 07416) in 20% FBS/PBS at 37 °C and rinsed with 5 mL FACS buffer. Bone pieces were digested again for 60 min in 1 mL of collagenase type I in 20% FBS/PBS and rinsed with 5 mL FACS buffer. Bone derived cells were collected from the supernatant and washed of both digestion buffers and then were plated at

a density of 2.2×10^4 cells/cm^2 in αMEM without ascorbic acid with 10% FBS and 1x P/S, or according to treatment conditions described below.

Cell culture maintenance

All marrow-derived and bone associated mesenchymal cell cultures were maintained in αMEM (without ascorbic acid) medium with 10% or 15% (for whole BM-derived stromal cells [BMSCs]) FBS and 1x P/S. Media changes were performed 5 d after initial plating, then every 2-3 d unless otherwise described. Cultures were incubated at 37 °C, 2% O_2, 5% CO_2. When cultures reached 80% confluence, media was removed and wells were washed twice with appropriate volumes of PBS. Adherent cells were dissociated by incubating each well with TrypLE Express Enzyme (Gibco, #12605010) at 37 °C for 3-5 min until cells have lifted from the plate surface. Tryp-LE dissociation was quenched by adding the equivalent volumes of αMEM (without ascorbic acid) with 10% FBS and 1x P/S to each well. Adherent cells were further dissociated by pipetting medium up and down over the well surface, and then cells were plated at a 1:3 split ratio. More details about the plate coating are available in supplemental information.

Magnetic depletion

CD45$^+$ cells were removed from marrow-derived cell cultures through magnetic selection. Cells were removed from culture plates by incubating each well with 0.5 mL of TrypLE Express for 3-5 min. TrypLE Express dissociation was quenched by adding 0.5 mL αMEM (without ascorbic acid) with 10% FBS and 1x P/S to each well. Cells were pelleted at 433xg for 5 min and surface stained with Biotinylated CD45 antibody (BD Pharmingen, Ref#553078, Clone 30-F11, 1:100 antibody dilution, 100 μL per 1×10^6 cells) for 25 min at 4 °C. Magnetic depletion was also used to enrich BSCs. For improved protocol for BSC culture, bone derived cells were surface stained with Biotinylated CD45 (BD Pharmingen, Ref#553078, Clone 30-F11), Ly6C (BD Pharmingen, Ref#557359, Clone AL-21), and F4/80 (eBioscience, Ref#123106, Clone BM8) antibodies at 5:100 antibody dilution, 100 μL per 1×10^6 cells for 25 min at 4 °C. Cells were washed with 1 mL FACS buffer, pelleted, then resuspended in streptavidin-magnetic bead particles (BD Biosciences) at 100 μL per 1×10^6 cells for 20 min at 4 °C. Media (αMEM (without ascorbic acid) with 10% FBS and 1x P/S) was added to each sample to equal 1 mL total volume, then samples were placed on a magnet for 4 min. Supernatant was collected and beads were resuspended in media (αMEM (without ascorbic acid) with 10% FBS and 1x P/S) and placed on the magnet for 4 min. This was repeated for a total of 4 times. Collected supernatant was placed on the magnet for 6 min, and final supernatant was collected.

Stromal cell differentiation

Stromal cells were differentiated along osteogenic, adipogenic, and chondrogenic pathways using standard methodologies previously described.[16] Detailed procedures are provided in supplemental information.

Light microscopy

Images were taken at room temperature using CKX41 inverted microscope (Olympus) and DP74 camera (Olympus). Cellsens software (Olympus) was used to acquire images on the microscope.

Lineage$^-$/Sca-1$^+$/c-kit$^+$ cells isolation

BM cells were flushed from tibias and femurs obtained from CD45.1 C57/B6 mice (8-12 wk old). The cells were stained with APC c-Kit$^+$ antibody and c-Kit$^+$ positive cells were enriched using anti-APC magnetic beads with auto MACS (Miltenyi Biotec). Subsequently, the cells were stained with a lineage antibody cocktail (PerCP Cy5.5 anti-B220, anti-Ter119, anti-CD3, and anti-Gr-1) and PE-CF594 anti-Sca-1) for 30 min at 4 °C. LSK cells were then purified using a FACS AriaII and plated into the designated plate for co-culture assay.

Stromal cell co-culture for competitive reconstitution assay

Seven thousand five hundred cells per well of sorted LSK cells were co-cultured in RPMI1640 (Corning, #10-041-CV) supplemented with 10% FBS, 1x P/S, and 1x 2-mercaptoethanol (Gibco, #21985023) with 80%-90% confluent layers of stromal cells in collagen-I coated 12-well plate at 37 °C, 5%CO_2, 2%O_2 for 3 days. The whole co-cultured cells were collected after trypsinization and mixed with 2×10^5 competitor cells (whole BM from 6 to 10 wk old CD45.2 C57/B6) in adjusted volume of 150 μL of PBS for transplantation.

Generation of chimeric mice (competitive reconstitution assay)

The BM transplantations were performed as previously described.[17] Chimeric (CD45.1/CD45.2 with or without GFP/UBC) mice were generated by transplantation of a designated number of BM cells into lethally irradiated (12 Gy, split dose) mice via tail veins. Reconstitution by donor cells was assessed in all mice by blood cell counts every month after injections, and chimerism of peripheral blood (PB) leukocytes was assessed by flow cytometry every 4 wk until 24 wk after transplantation. The proportion of PB leukocytes expressing CD45.1 or CD45.2 was determined monthly after transplantation by flow cytometry. The repopulating units (RUs) were evaluated using the standard formula: RU = % (C)/(100 − %), where % is the measured percentage of donor cells, and C is the number of competitor marrow cells per 1×10^5.[17,18]

RNA sequencing

Details are provided in supplemental information.

qPCR analysis

Details are provided in supplemental information.

ELISA and magnetic-based multi-immunoassay

Details are provided in supplemental information.

Immunohistochemistry staining

Details are described in supplemental information.

Statistical analysis

All data were expressed as mean ± SE of the mean. All analyses were made with GraphPad Prism software using two-tailed Student's *t*-test, Mann–Whitney nonparametric testing,

one-way ANOVA with Tukey's multiple-comparison post-test or Fisher's LSD test, and two-way ANOVA or mixed-model analysis with Geiser-Greenhouse correction applied when appropriate. Correlation analysis was done by nonparametric Spearman correlation. Exponential decay analysis was performed (one phase decay), half-life estimate was used to suggest a threshold. p-value <.05 was considered significant and denoted by asterisks ($^{*}p < .05$, $^{**}p < .01$, $^{***}p < .001$). RNA sequencing data were adjusted p-value (q) <0.05 was considered significant and denoted by asterisks ($^{*}q < 0.05$, $^{**}q < 0.01$, $^{***}q < 0.001$).

Detailed procedures for the statistics are also described in figure legends.

Additional information is provided in Supplementary Materials.

Results

Evaluation of previous strategies to maintain highly purified stromal cells ex vivo reveals persistent contamination of macrophages

We carefully evaluated the presence of contaminating CD45$^+$ cells in mouse BM-derived primary stromal cells (BMSCs) grown in vitro using protocols designed to maintain highly purified BMSCs.[19] Surprisingly, we found significant contamination of CD45$^+$ cells in the culture until passage 3 even in a 2D culture with collagen-I coated plates (Figure 1A). Another culture method that utilizes collagenase-I digested bones to isolate bone-associated stromal cells (BSCs) from murine hind limbs also resulted in significant contamination with CD45$^+$ cells (Figure 1B). For both BMSC and BSCs, CD45$^+$ cells represented more than 50% of the cultured cells. Flow cytometric analysis revealed that regardless of whether BM-derived or bone-derived, a majority of these CD45$^+$ cells were CD45$^+$/CD11b$^+$/Ly6G-/Ly6C-/F4/80$^+$ macrophages that highly expressed CD206 (Figure 1C), a M2 polarization marker.[20] CD45$^+$ macrophages (dark red arrow, population labeled in dark red in Figure 1C) were found in much smaller distribution in SSC-FSC plots compared to CD45$^-$ cells (Figure 1C), potentially leading to being disregarded in flow cytometric assessment of contamination. Most CD45$^-$ cells were CD31$^-$/Sca-1$^+$/CD51$^+$, consistent with stromal cells as previously described,[6] regardless of whether they were derived from BM or bone (Figure 1C). We then evaluated other previously reported strategies[11] that alter timing of first or subsequent cell passage to obtain highly purified stromal cells from BM cells (Figure S1A and B). However, in both cases we found persistent significant macrophage contamination of stromal cell cultures (Figure S1C and D). Next, we evaluated the efficacy of removing macrophages using magnetic particles (Figure S1E).[21] While targeted magnetic depletion reduced CD45$^+$ cell contamination in both BM and Bone-derived cultures, it did not eliminate it (Figure S1F and G). To obtain highly purified BMSCs, we plated BM cells and rather than passaging them, we sorted BMSCs as previously reported[19] by using a conventional gating strategy (CD45$^-$/Lin$^-$/CD31$^-$/Sca-1$^+$/CD51$^+$), plating the sorted cells. However, even after sorting, CD45$^+$ macrophages appeared in this culture after several days (Figure 1D). Given the positive correlation between the intensity of antigen expression of CD45 and of Ly6C/F4/80 (Figure 1E), we hypothesized that monocytes and macrophage progenitors with dim Ly6C/F4/80 expression concealed in the CD45$^-$ population may give rise to CD45$^+$ mature macrophages later in the culture.

Elimination of macrophages from ex vivo culture by targeting CD45$^+$/F4/80$^+$/Ly6C$^+$ cells

To determine the source of macrophage contamination in BMSCs, we sorted F4/80$^+$, Ly6C$^+$, and F4/80$^-$/Ly6C$^-$ populations from the CD45$^-$/Lin$^-$/CD31$^-$ cells, partially adopting a previously published procedure[19] (Figure 2A and B). When plated after sorting, F4/80$^+$ and Ly6C$^+$ cells showed significant contamination of CD45$^+$ cells (Figure S2A). In contrast, Ly6C$^-$/F4/80$^-$ sorted cells showed very small CD45$^+$ cell contamination (Figure S2A), suggesting that F4/80$^+$/Ly6C$^+$ cells in the CD45$^-$/Lin$^-$ population may include macrophage progenitors despite the low expression of CD45. Since this sorting strategy (CD45$^-$/Lin$^-$/CD31$^-$/Ly6C$^-$/F4/80$^-$/Sca-1$^+$/CD51$^+$) still had small residuals of macrophage contamination when using normal coated plate, we switched to collagen-I coated plates from the beginning of the process throughout the sorting and following passaging, which greatly improved the elimination of the macrophages from the culture after sorting (Figure 2C). Light microscopy visualization of non-sorted stromal cell cultures showed large cells with a fibroblastic pattern and smaller spindle-shaped cells that were absent in sorted cell cultures, suggesting that these smaller spindle-shaped cells are contaminating CD45$^+$ macrophages (Figure S2B and C), which were confirmed to be positive for F4/80 by immunohistochemistry staining while the back ground larger cell populations were not positive for F4/80 (Figure S2D). Since there is less macrophage contamination with bone sources, we adopted magnetic depletion using CD45$^+$/Ly6C$^+$/F4/80$^+$ to eliminate macrophages from BSCs (Figure 2A). CD45$^+$/Ly6C$^+$/F4/80$^+$ cell depletion significantly decreased macrophage contamination in the culture compared to CD45$^+$ single or CD45$^+$/F4/80$^+$ double targeting magnetic depletion (Figure 2D). However, macrophages reemerged in later passages (P2 or higher). Thus, we optimized the depletion process by titrating the primary antibody at the concentration of 1 μL per 1×10^6 cells and 5 μL per 1×10^6 cells. A primary antibody concentration at 5 μL per 1×10^6 cells throughout every passage from P0 to P3 completely eliminated CD45$^+$ macrophages (Figure 2E). In contrast to BMSCs, purified BSCs were morphologically heterogeneous, with a mixture of fibroblastic and cuboidal cells but lacking the smaller spindle-shaped cells, consistent with the elimination of macrophage contamination (Figure S2C). In summary, we have devised two distinct procedures that increase purity of stromal cell cultures derived from bone or BM by eliminating macrophage contamination.

Evaluation of the characteristics of stromal cells from BM and bones with or without macrophages reveals distinct signatures based on tissue of origin and macrophage contamination

To identify the characteristics of BM-derived and bone-derived cells, we performed RNA sequencing of ex vivo expanded stromal cells with (BMSC and BSC), or without (=enriched BMSC (E-BMSC) and enriched BSC (E-BSC)) macrophage contamination. Principal component analysis (PCA) and heatmap of differential gene expression showed clear separation of these 4 groups (Figure 3A and B).

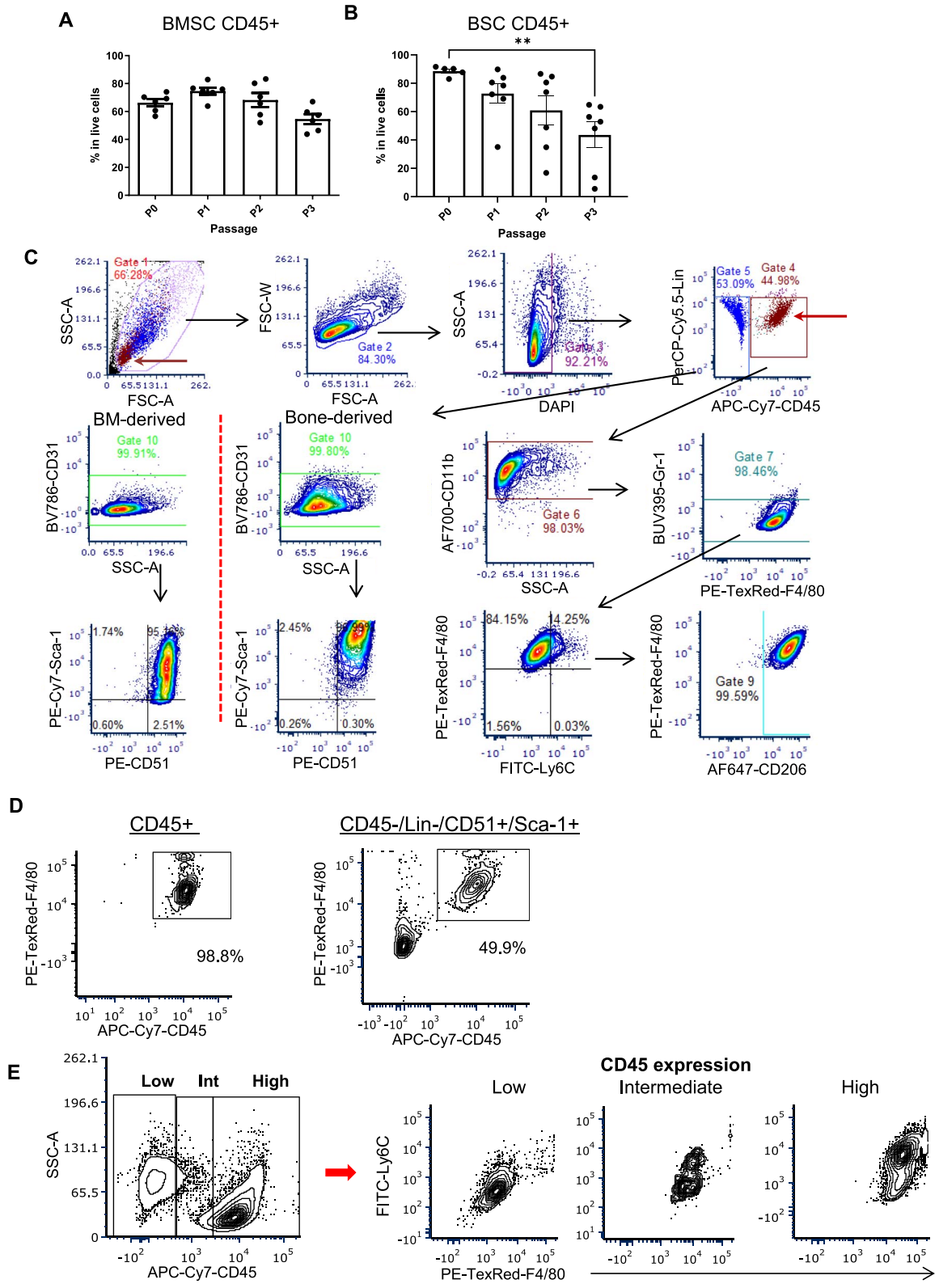

Figure 1. Persistent contamination of macrophages to stromal cells cultured in vitro. (A) The percentages of contamination with CD45 positive cell after multiple passages of mouse stromal cells from BM utilizing the previous reported methods and (B) BSCs from collagenase-I digested bones with collagen type I coating plates ($n = 6$-7, each dot represents independent mouse). Mean ± SEM, one-way ANOVA with Turkey's post-test are provided. *: $p < .05$; **: $p < .01$; ***: $p < .001$. (C) The representative gating scheme of the evaluation of macrophage contamination and stromal cell identification in cell cultures from BM and bones. Red arrow is pointing the highlighted quadrant in rightmost panel showing distribution of $CD45^+$ population (red brown) in FSC/SSC gate. (D) Representative flow cytometric analysis data of BM-derived cells 5 d after sorting. $CD45^+$ and $CD45^-/Lin^-/Sca\text{-}1^+/CD51^+$ sorted cells are displayed. (E) Representative flow cytometric data of day 5 $CD45^-/Lin^-/Sca\text{-}1^+/CD51^+$ sorted fraction showing the continual shift of intensity of F4/80 positivity along with the $CD45^+$ intensity.

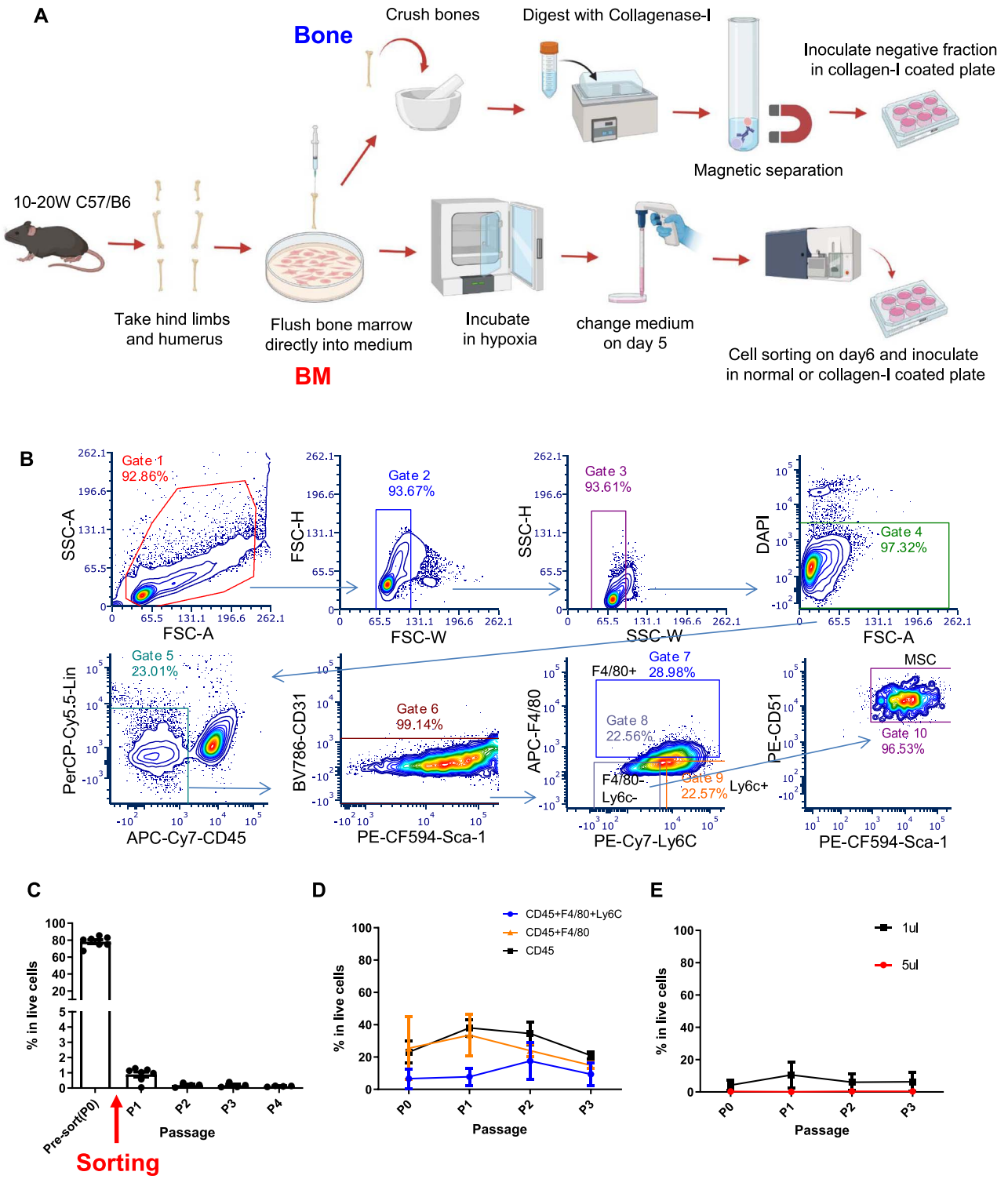

Figure 2. Successful depletion of hematopoietic cells by targeting CD45$^+$/F4/80$^+$/Ly6C$^+$ of mouse BM-derived and bone-derived stromal cells. (A) Schematic figure of the method for enrichment of stromal cells from BM and bones. (B) Representative gating plots for sorting of mouse BMSCs. (C) CD45$^+$ contamination (%) of the BM-derived cell culture from primary plating (P0) to passaging after sorting (passage: P1-P4). Each dot represents each mouse ($n = 4$). (D) CD45$^+$ contamination (%) of bone-derived cells after magnetic depletion by CD45, CD45/F4/80, and CD45/F4/80/Ly6C, $n = 3$. (E) CD45$^+$ contribution (%) of BAC-derived cells after magnetic depletion by CD45/F/4/80/Ly6C at primary antibody concentration of 1 μL/10e6 cells or 5 μL/10e6 cells, $n = 3$. (D, E): Passages 0 (initial plating) to 3 (P0-P3) are shown. Mean ± SEM are provided in (C), (D), and (E).

Lack of expression of *Ptprc* (CD45), *Itgam* (CD11b), and *Adgre1* (F4/80) in E-BSCs and E-BMSCs compared to control cultures confirmed their very high purity (Figure S3A). The proliferation marker *Mki67* (Ki-67) was highly expressed in BSC, BMSC, and E-BMSC, whereas E-BSC showed significantly lower *Mki67* expression (Figure 3C), suggesting that contaminating macrophages are directly or indirectly responsible for the high proliferation rate in BSCs.

Consistent with this, E-BMSC showed a rapid expansion in *ex vivo* culture compared to E-BSC (Figure 3D). As expected, differentiation markers, such as osteogenic marker *SP7* (Osterix), adipogenic marker *Adipoq* (Adiponectin), and chondrogenic marker *Sox9*, were higher in purified stromal cell culture (E-BSC/E-BMSC). However, each population showed different cell composition based on the cell source. There was higher *SP7* expression within the BMSCs, indicating the presence of osteoprogenitors, and higher *Sox9* expression within the BSCs, indicating the presence of early chondrogenic cells (Figure 3E). Additionally, *Spp1* (Osteopontin) expression was increased and *Sp7* expression was decreased in BSC (Figure 3E). Moreover, BSCs showed strong alkaline phosphatase activity at baseline but this expression was weaker in E-BSC (Figure 3F) suggesting that bone-derived cells represent a more differentiated osteolineage progenitor that may receive supportive signals by macrophages to stay in the osteoprogenitor state. The presence of more mature osteoblastic and chondroblastic cells in the BSCs, even in the absence of differentiating conditions, was highly influenced by the percentage of contaminating hematopoietic cells, as would be expected (Figure 3G and H). The expression patterns of periosteal markers, such as *Postn* (Periostin), *Ptgs2* (Cox-2), and *Ctsk* (Cathepsin K), indicated that E-BSC- and BM-derived cells did not have significant contamination with periosteal cells, whereas BSC showed significant increase of *Postn* and *Ptgs2* (Figure S3B). These data indicate that macrophage contamination to the culture may support carry-over periosteal cell ex vivo only for cell preparations from bone. Collectively these findings suggest that macrophages significantly impact stromal cell composition in ex vivo culture systems in ways that depend on tissue sources.

Macrophage contamination impacts differentiation potential of stromal cells from bone and marrow

Next, we tested impact of contaminating macrophages on stromal cell differentiation capacity. We assessed and quantified differentiation both using image quantification, and by measuring transcriptional markers of differentiation. Overall, BMSC and BSC have the ability to differentiate into three lineages, even in the presence of macrophages in the culture. Consistent with their transcriptional signature, BSCs and E-BSCs show stronger differentiation toward the chondrogenic lineage (Figure 4). However, macrophage contamination significantly disrupts the differentiation capacity of both BMSC and BSCs to all 3 lineages (Figure 4A and B). We further examined the influence of macrophage contamination to the culture on the differentiation capacity by assessing the relationship between the degree of macrophage contamination (percent of $CD45^+$ cells) examined by flow cytometric analysis and differentiation capacity measured via induction efficiency and expression of differentiation markers for each lineage. The ability of BSCs to differentiate to chondrocytes was significantly inversely correlated to the degree of $CD45^+$ cell contamination, as shown both by differentiation efficiency and by expression of differentiation markers (Figure 4A-C), however no specific threshold could be calculated. For both BSCs and BMSCs, the ability to differentiate to the osteoblastic lineage was significantly inversely correlated with the presence of $CD45^+$ cells (Figure 4D-F, Figure S3C). For BSCs, using the exponential decay equation, we could calculate a potential threshold (BSC osteogenic threshold: 5.070%, Figure 4E). Finally, adipogenic differentiation was exquisitely sensitive to macrophage contamination, as shown by significant inverse correlation of differentiation metrics to percent $CD45^+$ cells (Figure 4G-I, Figure S3D), and by the identification of very low calculated thresholds of $CD45^+$ cell contamination being sufficient to significantly inhibit adipogenic differentiation for both BSCs and BMSCs ((BSC: 0.5197%, BMSC: 3.731%, Figure 4H). Together, these data demonstrate the strong disruptive effects of macrophage contamination on differentiation capacity of cells derived from bone and BM.

SOX9/CD140a expression patterns confirm high purification of stromal cells from BM and bone and both were decreased by macrophage contamination

To further define the stromal cell characteristics of BM and bone derived cells, we focused on SOX9 expression. While SOX9 is an important transcriptional factor for chondrogenic differentiation, *Cre* recombinase activity targeted by the SOX9 promoter was previously shown to identify undifferentiated precursors that can differentiate to tri-lineage subsets and CXCL12-expressing stromal cells.[22] To evaluate SOX9 expressions in the murine BMME cells we isolated from BM or bone, we utilized SOX9-GFP transgenic mice. SOX9 expressing cells were rare in whole BM cells but could be detected in bone-derived cells (Figure 5A). $SOX9^+$ cells were enriched in the $CD45^-/Lin^-/CD31^-/CD51^+$ population and also detected in immature hematopoietic supportive cell populations like PαS ($Lin^-/CD45^-/CD31^-/Sca\text{-}1^+/CD140a^+$)[4] and Pααv ($Lin^-/CD45^-/CD31^-/CD51^+/CD140a^+$)[5] (Figure 5B). Next, we analyzed SOX9 expression in our ex vivo culture. Within $Lin^-/CD45^-/CD31^-/Sca1^+/CD51^+$ cells, E-BMSC and E-BSC showed higher expression of SOX9 compared to BMSC and BSC, and bone-derived cells showed relatively higher expression of SOX9 compared to BM-derived cells although it was not statistically significant (Figure 5C). Interestingly, the presence of $CD45^+$ cells and SOX9 expression had significant negative correlation in both BM- and bone-derived cells (Figure 5C). Consistent with this, CD140a (PDGFRα), a marker of HSC-supportive stromal cells,[4,5] was also highly expressed with both E-BMSC and E-BSC and was significantly reduced by macrophage contamination (Figure 4D). Collectively, these results confirm that our strategy for ex vivo purification of stromal cells could successfully extract very rare, immature and critical stromal components from both BM and bone, and that macrophage contamination could alter the characteristics of these cells.

Enriched stromal cell cultures have improved ability to support hematopoietic cells

Next, we examined the ability of our ex vivo cultures to support hematopoiesis. To test this, we developed an ex vivo co-culture system of stromal cells and BM HSC-enriched $Lin^-/Sca\text{-}1^+/c\text{-}Kit^+$ cells (LSKs) without growth factors in hypoxic (2% O_2) conditions and analyzed stromal cells' supporting effect on short- and long-term repopulation of hematopoietic cells as evaluated by competitive reconstitution assays, the gold standard for HSC function (Figure 6A). Both BM and BSCs showed significantly higher chimerism of co-cultured cells ($CD45.1^+$) in PB compared to LSKs

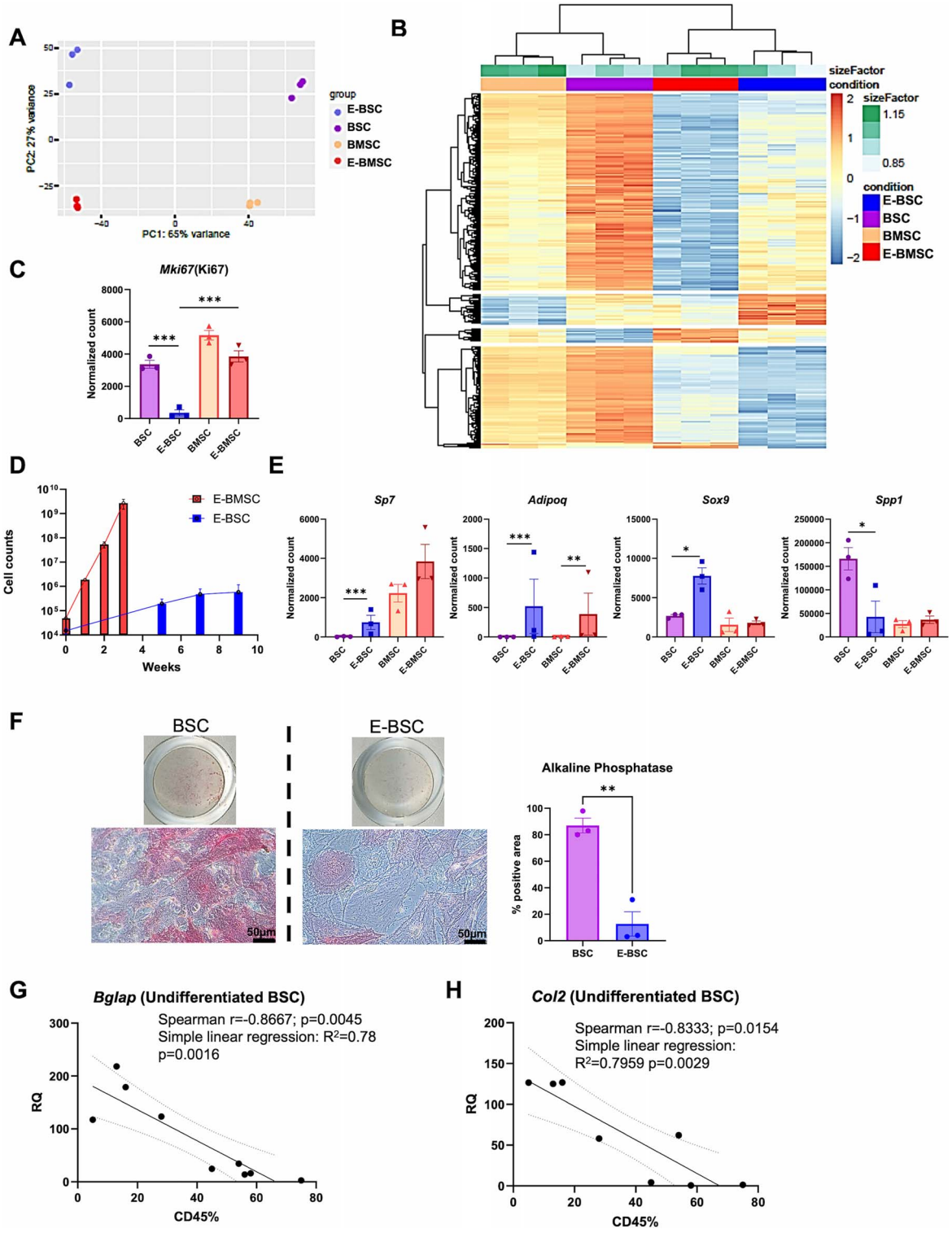

Figure 3. Transcriptional and functional analyses of BM- and bone-derived cells with or without macrophages. (A) Principal component analysis (PCA) plot of BSC/E-BSC (enriched-BSC)/BMSC/E-BMSC (enriched-BMSC). Each dot represents 3 independent mouse samples. (B) Hierarchical clustering heat map of the set of differentially expressed genes. E-BSC (blue) vs BSC (purple) vs BMSC (Orange) vs E-BMSC (red) samples scaled per gene, $n = 3$. (C) Normalized counts of *Mki67*(Ki67) gene expression. Each dot represents samples from each mouse, $n = 3$. (D) Expansion curve of E-BMSC and E-BSC with passaging until passage 3, $n = 3$-6. (E) Normalized counts of *Sp7* (Osterix), *Adipoq* (Adiponectin), *Sox9*, and *Spp1* (Osteopontin) genes expression. Each dot represents samples from each mouse, n = 3. (F). Representative images of photograph and light microscopy of bone-derived cells (BSC: Left, E-BSC: Right) at day 14 with non-differentiation medium with alkaline phosphatase/Von Kossa double staining (scale bar = 50 μm) and %positive for alkaline phosphatase staining calculated by BZ-X software are presented ($n = 3$). (G, H) Correlation analysis of expression of *Bglap* (G) and *Col2* genes (H) in undifferentiated co-cultures measured by qPCR (RQ calculated based on E-BMSC expression) with %CD45$^+$ cells present in each culture based on flow cytometric analysis. Each dot represents an individual co-culture. Correlation analysis between CD45% and RQ was done by nonparametric spearman correlation analysis. $n = 8$-9. Simple linear regression analysis was performed, 95% confidence interval boundaries are shown by the dotted lines. Mean ± SEM, in (C), (D), and (E), adjusted p(q) in (C) and (E) and Student *t*-test (*p*) in (F) are provided. *: $q < 0.05$; **: $q < 0.01$; ***: $q < 0.001$.

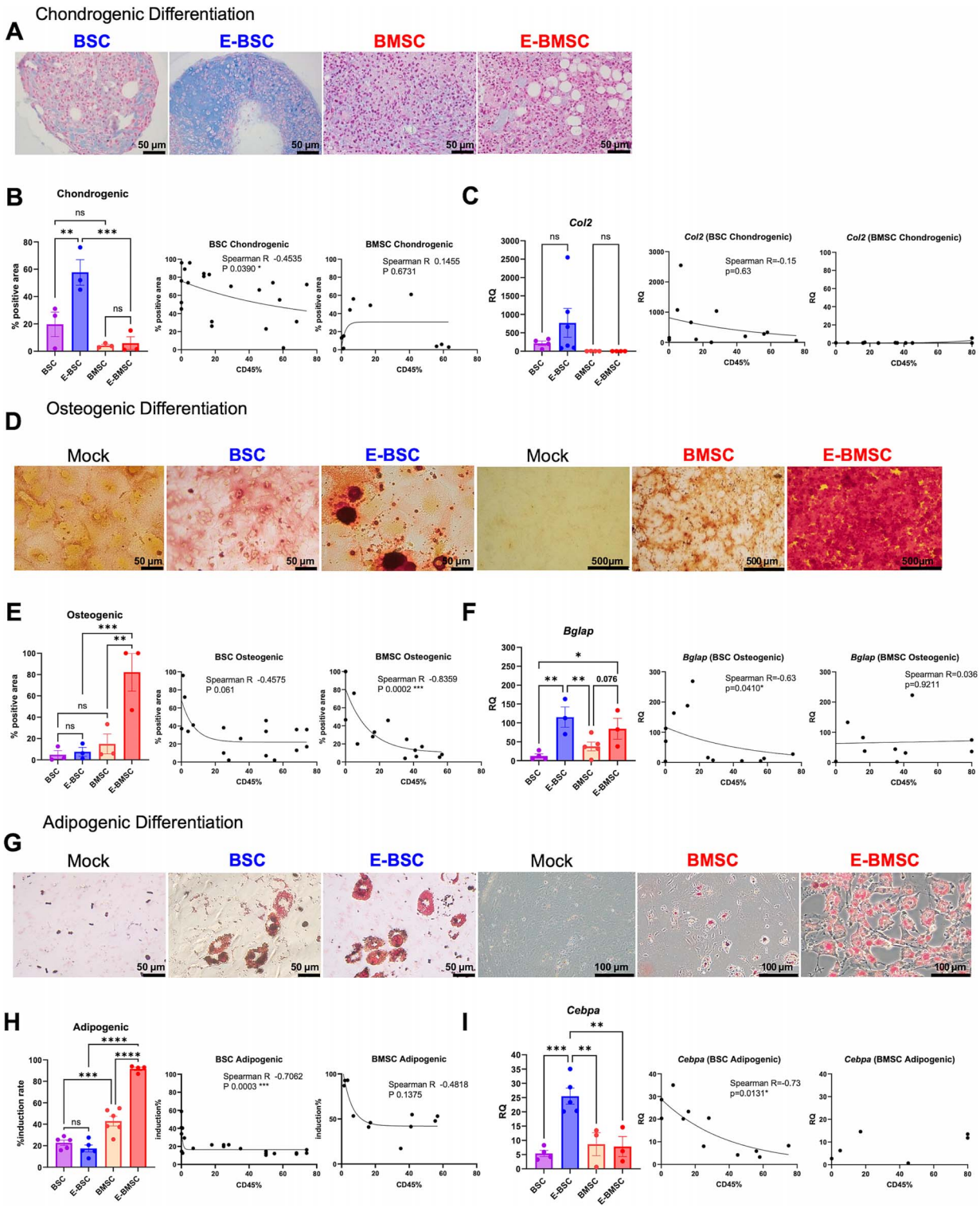

Figure 4. Quantification of differentiation analysis of BM- and bone-derived cells with or without macrophages. Comparison of trilineage differentiation capacity of each group (BSC/E-BSC/BMSC/E-BMSC). (A, D, G): Representative images of tri-lineage differentiation for cell populations as labeled Alcian blue staining with chondrogenic differentiation (A), alizarin red staining with osteogenic differentiation (D) and oil-red-O staining with adipogenic differentiation (G) are shown. Mock: Normal medium with no differentiation factors. (B, E, H): Induction rate calculated by %positive area calculated by BZ-X software with Alcian blue in chondrogenic differentiation (B), alizarin red in osteogenic differentiation (E), and % oil-red-O positive cells in adipogenic differentiation (H), are presented. $n = 3$-5. (C, F, I) qPCR analysis of mRNA of expressed gene in control/induced BSC/E-BSC, BMSC/E-BMSC cultures in the chondrogenic (C), osteogenic (F), and adipogenic (I) differentiation conditions. Relative expression/internal control are presented. $n = 3$-5. (B, C, E, F, H, I) Correlation analysis and exponential decay equation analysis between %$CD45^+$ cells and lineage differentiation capacity calculated for each procedure (Chodrogenic, (B): %positive area, osteogenic, (E): %positive area, adipogenic, (H): % induction rate) and differentiation marker expression (C, F, I) on BMSC and BSC. Correlation analysis between CD45% and %positive area, % induction rate or RQ was done by nonparametric Spearman correlation analysis. Mean ± SEM, in (B), (C), (E), (F), (H), and (I), one-way ANOVA with uncorrected Fisher's LSD (p) in (B), (C), (E), (F), (H), and (I) are provided. *: $p < .05$; **: $p < .01$; ***: $p < .001$; **** < $p < .0001$.

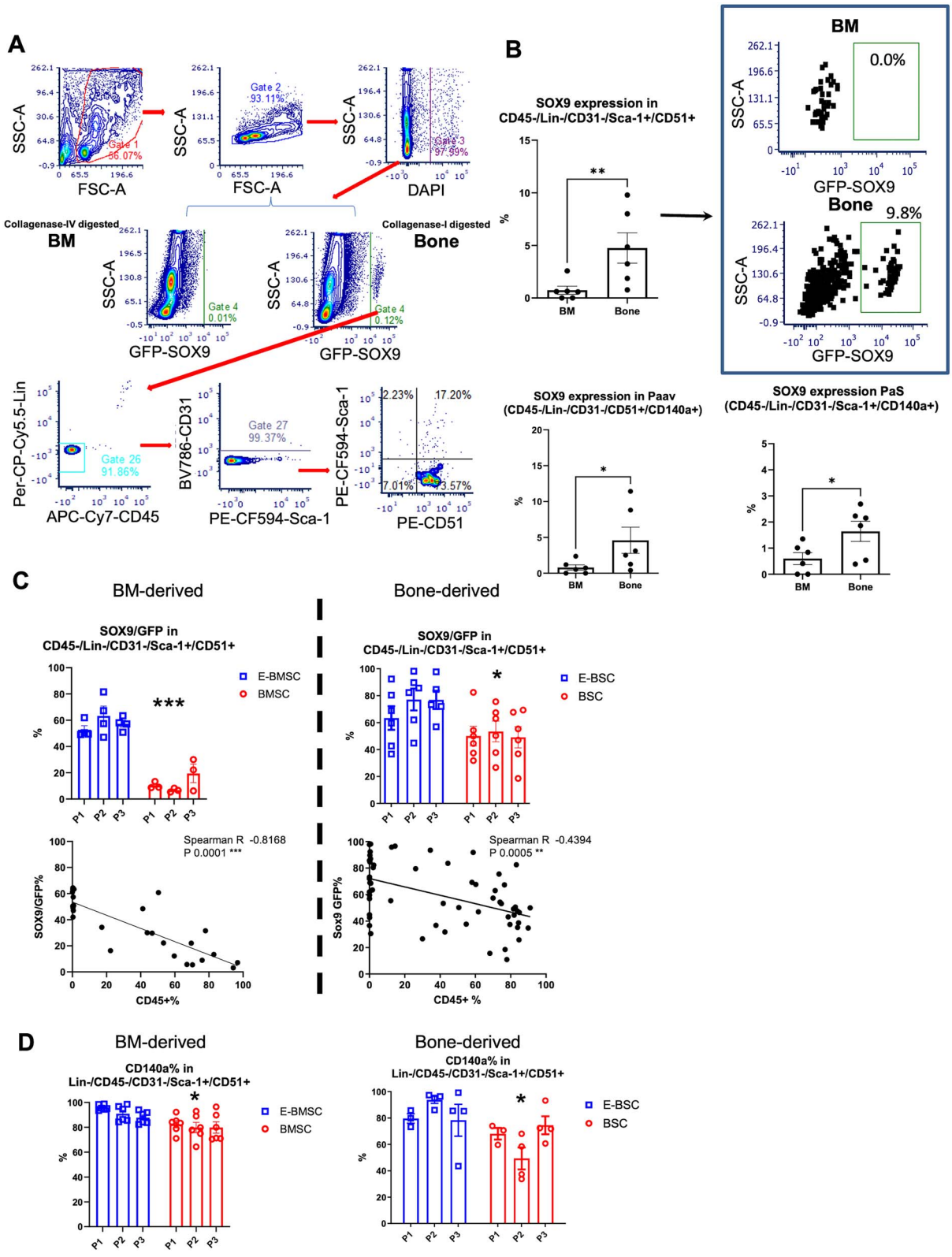

Figure 5. Sox-9/CD140a expression patterns confirmed high purification of stromal cells from BM and bones and both are affected by macrophage contamination. (A) Representative gating plot of collagenase-IV digested BM or collagenase-I digested bones for the expression patterns of SOX9-GFP. (B) SOX9-GFP expression (%) in stromal cells ($CD45^-/Lin^-/CD31^-/Sca\text{-}1^+/CD51^+$), PαS and Pααv, and representative dot plot patterns of Sox9-GFP expression in stromal cell fraction. Each dot represents each mouse, $n = 4$ (C). SOX9-GFP positive% in stromal cell fraction along with the passaging and correlation plot between $CD45^+$ (%) and $SOX9^+$ (% in stromal cells) of BM-derived (left) and bone-derived (right). $n = 3$-6, $n = 26$-59, each dot represents each sample from an individual mouse in bar graph. (D) $CD140a^+$ (%) in stromal cell fraction along with the passaging of BM-derived (left) and bone-derived (right). $n = 4$-6, each dot represents each sample from an individual mouse. Mean ± SEM, Student *t*-test for (B), mixed-model analysis with Geiser-Greenhouse correction for (C) and (D), correlation analysis for (C) is provided. *: $p < .05$; **: $p < .01$; ***: $p < .001$.

without stromal support (Figure 6B, Figure S4A). The BMSC displayed both early (4 wk) and long term (24 wk) disruption of reconstitution measured by direct engraftment and reconstitution units (Figure 6C), demonstrating that the presence of macrophages in BMSC cultures obscures functional assessment of microenvironmental support of HSPCs by stromal cells. Macrophage contamination differentially impacted the ability HSPCs to contribute to mature hematopoietic cell populations in PB. Macrophage presence in BMSC disrupted donor contribution of $B220^+$ cells (Figure 6D). In contrast, in BSCs, macrophage presence induced myeloid cell expansion (Figure S4B). When we examined BM reconstitution at 24 wk post-transplantation, macrophage contamination in BMSC co-cultures decreased contribution to the lymphoid populations, such as T-cells ($CD11b^-/CD3e^+$), lymphoid progenitors (MPP4: Lin^-/c-Kit^+/$Sca\text{-}1^+$/$Flt3^+$/$CD48^+$/$CD150^-$), and HSCs (short-term(ST)-HSC: Lin^-/c-Kit^+/$Sca\text{-}1^+$/$Flt3^-$/$CD48^-$/$CD150^-$ and long-term (LT)-HSC: Lin^-/c-Kit^+/$Sca\text{-}1^+$/$Flt3^-$/$CD48^-$/$CD150^+$)[6,23] (Figures S4C and S6E, Figure S5A). In spite of the lack of impact of macrophage contamination in BSCs PB reconstitution, LSKs co-cultures with BSC had significant decline in contribution to lymphoid progenitors, MPP4s and myeloid progenitors (CMP; (common myeloid progenitor:Lin^-/c-Kit^+/$Sca\text{-}1^-$/$CD34^+$/$CD16/32^-$) and MPP2 (Lin^-/c-Kit^+/$Sca\text{-}1^+$/$Flt3^-$/$CD48^+$/$CD150^+$)) (Figures S4C, D and S5A), suggesting subtle skewing of HSC function induced by the presence of macrophages in BSCs. These findings clearly show that macrophage contamination to stromal cell culture disrupts their ability to support hematopoiesis, and that macrophages derived from different tissues have distinct effects on stromal support of hematopoiesis (Figure S5B).

To identify candidate factors that disrupt the stromal support of hematopoiesis when macrophages are present in the co-culture, we further analyzed the RNA sequencing data for the key markers of hematopoietic support. *CXCL12, ANGPT1,* and *KITLG* were decreased by macrophage contamination to both bone and BM derived stromal cells (Figure 7A). *VCAM1*, one of the representative markers of the known critical niche component, Leptin $receptor^+$ cells[24,25] was highly expressed in all stromal cells, but especially in E-BSC (Figure 7A). Together with the decreases in SOX9 and CD140a expression in stromal cells induced by macrophage contribution (Figure 5C and D), these transcriptional changes may contribute to how the presence of macrophages disrupts the ability of BM- and bone-derived stromal cells to support hematopoiesis ex vivo. To determine which factors from macrophages could drive the defect in hematopoiesis, we analyzed the transcriptomes of the enriched and macrophage contaminated cultures. We found that expression of inflammatory chemokines was increased in cultures that included macrophages, especially with BSCs (Figure 7B). This, in addition to the higher expression of inflammatory signals already reported to induce myeloid skewing of HSCs (*Il1b*, *Ccl3*, and *Cxcl2*, Figure S6A) could partially explain the myeloid skewing and reduction of myeloid progenitors with BSCs co-cultured LSKs identified by the competitive reconstitution assay (Figure S4A and B). The protein level of these myeloid chemoattractant, such as CCL3 and CXCL2 in the supernatant of stromal cell culture examined by magnetic-based multi-immunoassay were higher in BSCs, which were consistent with the transcriptional profile of transcriptomes (Figure 7C). In addition, RNA level of the complement subcomponents *C1qa* and *C1qc* were highly expressed in macrophage contributed culture (BMSC, BSC) in contrast to enriched stromal cells (E-BMSC, E-BSC) (Figure S6B), and the protein level of C1q was much higher with macrophages contributed culture confirmed by ELISA (Figure 7D). Collectively, these results indicate that macrophage contamination in these cultures could have both a direct impact on HSCs via chemokine/cytokine production as well as an indirect effect via altered stromal cell characteristics.

Discussion

Stromal cells can technically be isolated and sorted from human and murine tissues, but these cells are heterogeneous and extremely limited in number (estimated at 0.001%-0.01% of marrow nucleated cells[26]). The methodology to isolate highly purified functional primary stromal cells has long been a subject of controversy but is essential, since stromal cell purification is indispensable to precisely recapitulate their functional roles in BMME to explore their role in hematopoiesis, inflammatory states, and hematological malignancies. There are several previous methodological reports regarding ex vivo culture of primary mouse stromal cells.[11,12,19] However, these methods appear to underestimate the macrophage contamination in the cultures. We found that the morphology of murine macrophages in ex vivo culture can be distinguishable from the much larger stromal cells based on cell size although both cell types strongly adhere to the plastic surface and are inseparable with conventional trypsinization (Figure S2B-D). We suspect that significant macrophage contamination of stromal cell cultures may be inadvertently missed because macrophages are very small compared to stromal cells and therefore are primarily found in low forward scatter (FSC) and side scatter (SSC) cell populations, as we show in this study (Figure 1C). The persistent macrophage contamination in stromal cell cultures seems to be a hallmark of mouse in contrast to human stromal cells, where we can achieve a high purity with a conventional method by plating BM mononuclear cells in adherent plates under high serum conditions.[27–29] While cell sorting can be generally adopted to deplete the hematopoietic cells to enrich rare cell populations, we found that a stringent gating strategy is required to eliminate monocyte/macrophage progenitors in CD45/lineage negative populations. Importantly, myelomonocytic progenitors are likely present in CD45 dim populations. These progenitors enhance CD45 expressions as they differentiate to mature monocytes or macrophages,[30] likely explaining why monocyte/macrophage progenitors are not completely excluded based on the expression of CD45 for stromal cell enrichment. The protocols presented here highly enriched BMSCs and BSCs, reducing the macrophage contamination to 0%-1% ex vivo with a combination of stringent sorting or depletion and utilization of type I collagen (collagen-I) coated plates. Collagen-I, a fibrous protein rich in connective tissues, is the major component of extracellular matrix, and it could enhance the adhesion, survival, and proliferation of human cells that are grown in collagen-I coated plates.[31] We successfully attained rapid growth and improved enrichment rate of E-BMSCs with the support of collagen-I although growth speed of E-BSCs remained

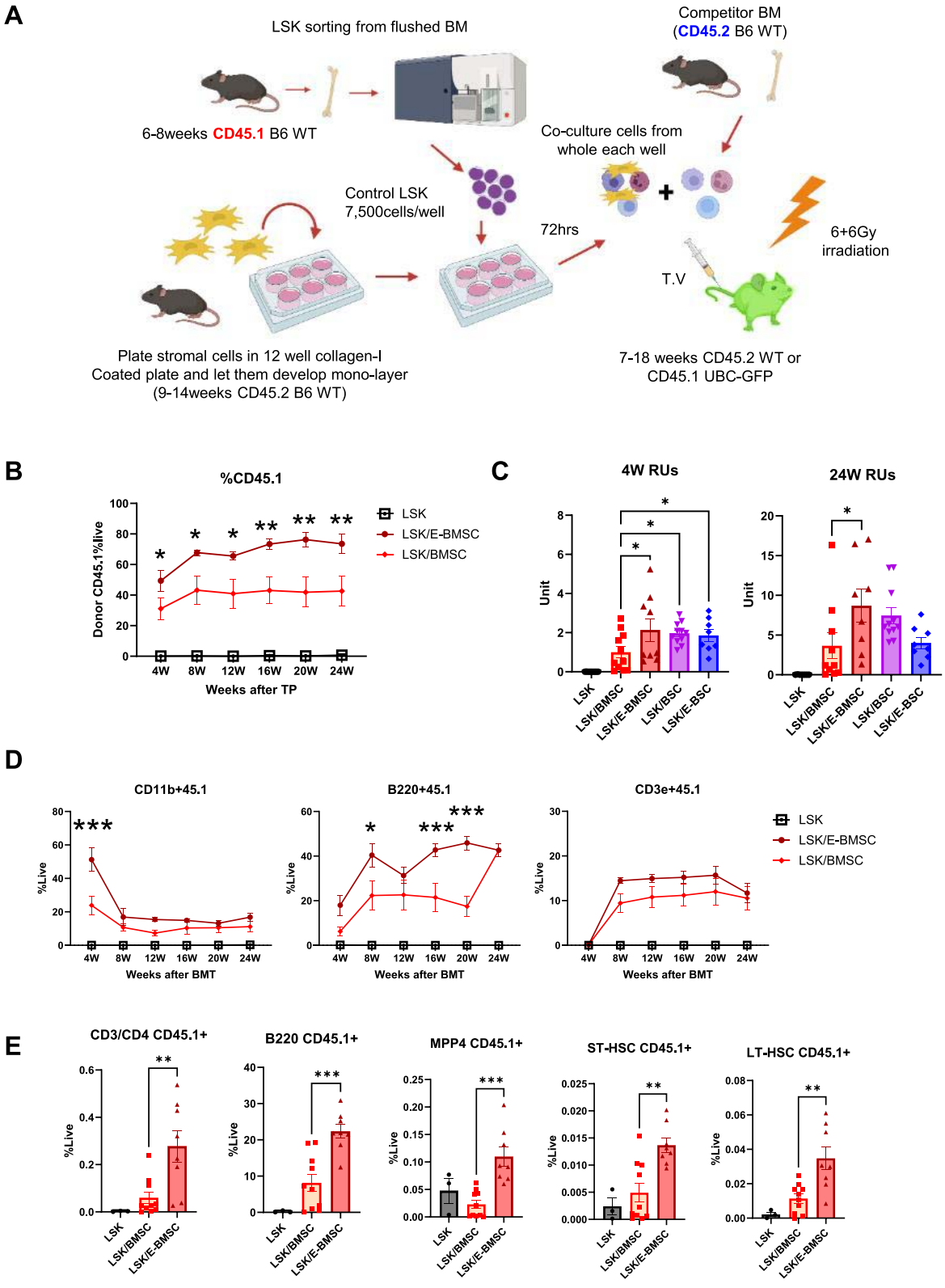

Figure 6. Purified stromal cell cultures have high ability to support hematopoietic stem and progenitor cells which is disrupted by macrophage contamination. (A) Schematic figure of competitive reconstitution assay with stromal cells and LSK cells co-culture. (B) Analysis of peripheral blood (PB) chimerism (CD45.1%) from LSKs transplanted after culture alone or co-cultured with BMSC or E-BMSC, $n = 5$-11. (C) Early (4 wk) and long-term (24 wk) reconstituting units (RUs) after transplantation, $n = 7$-11. (D) Myeloid ($CD11b^+$), B-cell ($CD11b^-/B220^+$), and T-cell ($CD11b^-/CD3e^+$) reconstitution (CD45.1%) in PB after transplantation of donor LSK alone or co-cultured with BMSC or E-BMSC as in (A), $n = 5$-11. (E) BM analysis at 24 wk after transplantation of LSKs alone or co-cultured LSKs with BMSC or E-BMSC, $n = 5$-11. Mean ± SEM, two-way ANOVA with Turkey's post-test for (B) and (D), one-way ANOVA with Turkey's post-test for (C) and (E) are provided. *: $p < .05$; **: $p < .01$; ***: $p < .001$.

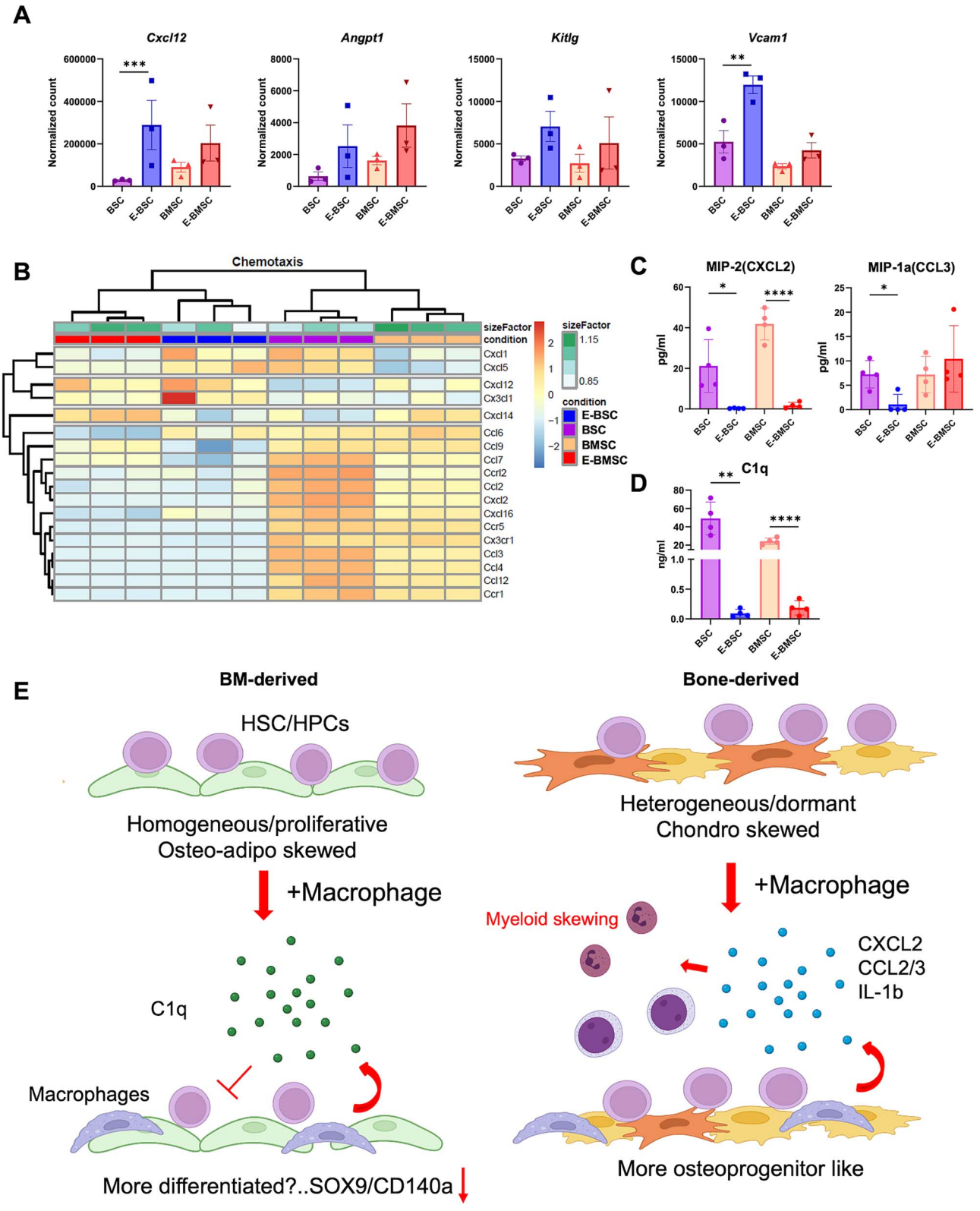

Figure 7. Macrophage presence in stromal cell cultures reduced expression of hematopoietic supporting factors and increased inflammatory factors in culture supernatant. (A) Normalized counts of transcriptional expression of *Cxcl12, Angpt-1, Kitl, Vcam-1* obtained by RNA-seq, $n = 3$. (B) Hierarchical clustering heat map of the set of differentially expressed genes of chemotaxis. E-BSC (blue) vs BSC (purple) vs BMSC (Orange) vs E-BMSC (red) samples scaled per gene, $n = 3$. (C) Protein level of MIP-2 (CXCL2), MIP-1a (CCL3) obtained by magnetic-based multi-immunoassay and (D) C1q obtained by ELISA. $n = 4$, each dot represents stromal cell samples derived from each mouse. (E) Schematic summary of differential characteristics of BM- and bone-derived stromal cells with or without macrophage contamination. Mean ± SEM, adjusted $p(q)$ in (A), Student t-test for (C) and (D) are provided. *: $q < 0.05$; **: $q < 0.01$; ***: $q < 0.001$. *: $p < .05$; **: $p < .01$; ***: $p < .001$; ****: $p < .0001$.

slow. A recent study showed that liposomal clodronate can efficiently reduce macrophage contamination in mouse BMSC cultures, allowing attainment of up to 95% purity of stromal cells.[32] However, clodronate induces cell death of macrophages, whereas our culture system achieves high purity of stromal cells without inducing cell death, a potential source for inflammatory signals which could also disrupt stromal function.

Our enriched stromal culture systems enabled us to demonstrate novel aspects of tissue-derived stromal cells. RNA sequencing data obtained from ex vivo cultures from two different sources with two different customized protocols (E-BSC/BSC/E-BMSC/BMSC) showed clear dissection of the stromal cells and macrophages from BM and Bones. Some of previous reports argued that stromal cells from different tissues could be characteristically different,[33] but these studies lacked the functional assessment of stromal cells ex vivo and the verification of stromal cell purity. In this study, stromal cells from different sources (Bone vs BM) are distinct transcriptionally and functionally, even though they are immunologically similar based on flow cytometric analysis. Importantly, enriched stromal cells showed enhanced ability to differentiate, revealing clear differences in lineage differentiation potential of BM- and bone-derived stromal cells. Notably, exponential decay equation analysis between macrophage contamination degree (CD45%) and differentiation capacity revealed that quite a high level of purity is required (at least $\leq$5% according to threshold calculations, Figure 4) to eliminate the disruptive effect of macrophages on differentiation capacity in both BM- and bone-derived cells. Moreover, macrophages from different tissues also showed differential effects on stromal cells transcriptionally and functionally. As shown in Figure 3E and F, macrophage contamination to bone derived cell cultures significantly alters the expression patterns of *SP7* (Osterix) and *SPP1* (Osteopontin) and the intensity of alkaline phosphatase activity at baseline. Since Osteopontin was reported to be enriched in pre-osteoblastic cells,[17,34] bone-derived macrophages might enhance preosteoblastic cell contribution to the stromal cell pool. We also established a novel co-culture system of hematopoietic cells and stromal cells. There are several previous reports performing ex vivo co-culture to evaluate the ability of stromal cells to support hematopoietic cells, however these required the addition of growth factors such as SCF and Flt3 for hematopoietic cell growth.[34,35] We reasoned that the inclusion of growth factors could underestimate and/or skew the effects of the stromal cells on HSPC cell fates. Our growth-factor-free co-culture system was feasible, yielding HSCs capable of competitive reconstitution, and it uncovered the differential ability of BM- and bone-derived stromal cells to support HSPCs. We also found that the hematopoietic supporting effects of stromal cells were significantly compromised by the presence of macrophages. These functional differences further highlight the impact of macrophage contamination, which should be evaluated and avoided in experiments investigating the roles of stromal cells as the HSC niche.

A major impact of the presence of macrophages was the induction of myeloid skewing in HSPCs. These data are highly consistent with our work demonstrating that aged macrophages are sufficient to induce HSPC skewing.[6] The transcriptomes and protein levels of myeloid chemoattractants, such as *CCL3* and *CXCL2*, were upregulated with BSCs. In addition, *IL1b* expression was much increased by BSCs, which might explain more severe myeloid skewing of HSPCs co-cultured with BSCs. Similarly, expression of *C1qa/C1qc* genes were increased in cultures containing macrophages, which were also confirmed by higher protein levels in culture supernatant. C1q is a major constituent of the complement system, which plays a critical role in immune defense, but also leads to aging of stem cells in multiple organs via activation of canonical Wnt signaling.[36] Excessive expression of C1q components in macrophage-including cultures may also impair HSPC function. These facts indicated possible mechanisms of macrophage-stromal cell crosstalk ex vivo that could explain the functional changes in stromal cells contaminated by macrophages while also reflecting in vivo macrophage-stromal cell interactions. The active production of inflammatory factors from macrophages in ex vivo culture with stromal cells as shown by RNA sequencing indicated that macrophages disturb stromal cells not simply with a dilution effect by numerically contributing to the culture (Figure 7E).

Several reports explore macrophage and stromal cell interactions and their impact on their differentiation potential and their immunomodulatory effects in vivo.[37] In addition to extending these findings, the current manuscript highlights the pleiotropic impact of macrophage contamination to the ex vivo stromal cell culture. Our culture system revealed that macrophages undergo skewing to a $CD206^+$ M2 phenotype regardless of their source, consistent with prior reports showing that stromal cells could drive activated inflammatory macrophages to M2 phenotype polarization in ex vivo culture[38] via cell–cell contact as well as through soluble factors including PGE2 and TGF-β produced by stromal cells.[39] Despite some limitations of the ex vivo culture system, we identify the differential effect of macrophages from different sources (BM and bones) on stromal cell function. Together, these findings strongly suggest that purity of BM- and bone-derived stromal cells is of the essence when experiments intend to study stromal cell characteristics and function. We speculate that some of the lack of consistency in studies on murine stromal cells may be due to underappreciated contribution of contaminating macrophages. Collectively, here we established highly purified ex vivo stromal cell culture systems from two different sources from BMME and provide strong evidence for the need not only to specify the source (BM vs bone) but also to achieve high purification without macrophage contamination for the accurate study of stromal cell function, differentiation and ability to support HSPCs, and interactions with macrophages within the BMME. These powerful methods could advance the identification of regulatory mechanisms that are critical to understand skeletal and hematopoietic interactions in homeostasis, development, aging, and hematopoietic disorders including malignancies.

Acknowledgments

The authors would like to thank Daniel Byun, Lizz LaMere, and Chunmo Chen for technical assistance, and the University of Rochester Flow Cytometry for their assistance. This work was performed with the assistance of the Flow Cytometry Core and the Genomics Research Center at Wilmot Cancer Institute and the University of Rochester School of Medicine and Dentistry.

Author contributions

H.K. and Y.K. designed the study, analyzed the data, and wrote the paper. Y.K., H.K., N.V., S.B., A.J.L., J.Z., E.R.Q., M.G., M.A., D.K.B., E.A.L., M.W.L. performed experiments. N.A.S. performed

bioinformatics analysis. J.L.L. and M.W.B. contributed to the interpretation of data. L.M.C. supervised the work, designed the research, and wrote the manuscript.

Supplementary material

Supplementary material is available at *JBMR Plus* online.

Funding

Funding for this work was supported by the National Institutes of Health under Grant P30 AR061307, the Edward P. Evans Foundation under Grant #005545 (to L.M.C.), Overseas Research Fellowship, Japanese Society for the Promotion of Science (JSPS) to Y.K., R01s AG079556 and AG076786. National Cancer Institute grant P30 CA272032.

Conflicts of interest

The authors declare no competing interests.

Data availability

The datasets used and/or analyzed during the current study are available from the corresponding authors. RNA sequence dataset is available via GEO Accession #GSE228749 (available with token for review). Resource availability: correspondence and requests for materials should be addressed to L.M.C.

References

1. Kolf CM, Cho E, Tuan RS. Mesenchymal stromal cells. Biology of adult mesenchymal stem cells: regulation of niche, self-renewal and differentiation. *Arthritis Res Ther*. 2007;9:204
2. Anjos-Afonso F, Siapati EK, Bonnet D. In vivo contribution of murine mesenchymal stem cells into multiple cell-types under minimal damage conditions. *J Cell Sci*. 2004;117:5655–5664. https://doi.org/10.1242/jcs.01488
3. Lv FJ, Tuan RS, Cheung KM, Leung VY. Concise review: the surface markers and identity of human mesenchymal stem cells. *Stem Cells*. 2014;32:1408–1419. https://doi.org/10.1002/stem.1681
4. Morikawa S, Mabuchi Y, Kubota Y, et al. Prospective identification, isolation, and systemic transplantation of multipotent mesenchymal stem cells in murine bone marrow. *J Exp Med*. 2009;206:2483–2496. https://doi.org/10.1084/jem.20091046
5. Pinho S, Lacombe J, Hanoun M, et al. PDGFRalpha and CD51 mark human nestin^{+} sphere-forming mesenchymal stem cells capable of hematopoietic progenitor cell expansion. *J Exp Med*. 2013;210:1351–1367. https://doi.org/10.1084/jem.20122252
6. Frisch BJ, Hoffman CM, Latchney SE, et al. Aged marrow macrophages expand platelet-biased hematopoietic stem cells via Interleukin1B. *JCI Insight*. 2019;5:1–20. https://doi.org/10.1172/jci.insight.124213
7. Balderman SR, Li AJ, Hoffman CM, et al. Targeting of the bone marrow microenvironment improves outcome in a murine model of myelodysplastic syndrome. *Blood*. 2016;127:616–625. https://doi.org/10.1182/blood-2015-06-653113
8. Anthony BA, Link DC. Regulation of hematopoietic stem cells by bone marrow stromal cells. *Trends Immunol*. 2014;35:32–37. https://doi.org/10.1016/j.it.2013.10.002
9. Geyh S, Oz S, Cadeddu RP, et al. Insufficient stromal support in MDS results from molecular and functional deficits of mesenchymal stromal cells. *Leukemia*. 2013;27:1841–1851. https://doi.org/10.1038/leu.2013.193.
10. Frisch BJ, Ashton JM, Xing L, Becker MW, Jordan CT, Calvi LM. Functional inhibition of osteoblastic cells in an in vivo mouse model of myeloid leukemia. *Blood*. 2012;119:540–550. https://doi.org/10.1182/blood-2011-04-348151
11. Soleimani M, Nadri S. A protocol for isolation and culture of mesenchymal stem cells from mouse bone marrow. *Nat Protoc*. 2009;4:102–106. https://doi.org/10.1038/nprot.2008.221
12. Baddoo M, Hill K, Wilkinson R, et al. Characterization of mesenchymal stem cells isolated from murine bone marrow by negative selection. *J Cell Biochem*. 2003;89:1235–1249
13. Pittenger MF, Mackay AM, Beck SC, et al. Multilineage potential of adult human mesenchymal stem cells. *Science*. 1999;284:143–147. https://doi.org/10.1126/science.284.5411.143
14. Yi X, Liu X, Kenney HM, et al. TNF-polarized macrophages produce insulin-like 6 peptide to stimulate bone formation in rheumatoid arthritis in mice. *J Bone Miner Res*. 2021;36:2426–2439. https://doi.org/10.1002/jbmr.4447
15. Kilkenny C, Browne WJ, Cuthill IC, Emerson M, Altman DG. Improving bioscience research reporting: the ARRIVE guidelines for reporting animal research. *PLoS Biol*. 2010;8:e1000412. https://doi.org/10.1371/journal.pbio.1000412
16. Azadniv M, Myers JR, McMurray HR, et al. Bone marrow mesenchymal stromal cells from acute myelogenous leukemia patients demonstrate adipogenic differentiation propensity with implications for leukemia cell support. *Leukemia*. 2020;34:391–403. https://doi.org/10.1038/s41375-019-0568-8
17. Kawano Y, Fukui C, Shinohara M, et al. G-CSF-induced sympathetic tone provokes fever and primes antimobilizing functions of neutrophils via PGE2. *Blood*. 2017;129:587–597. https://doi.org/10.1182/blood-2016-07-725754
18. Kawamori Y, Katayama Y, Asada N, et al. Role for vitamin D receptor in the neuronal control of the hematopoietic stem cell niche. *Blood*. 2010;116:5528–5535. https://doi.org/10.1182/blood-2010-04-279216
19. Huang S, Xu L, Sun Y, Wu T, Wang K, Li G. An improved protocol for isolation and culture of mesenchymal stem cells from mouse bone marrow. *J Orthop Translat*. 2015;3:26–33. https://doi.org/10.1016/j.jot.2014.07.005
20. Lawrence T, Natoli G. Transcriptional regulation of macrophage polarization: enabling diversity with identity. *Nat Rev Immunol*. 2011;11:750–761. https://doi.org/10.1038/nri3088
21. Schneider S, Rusconi S. Magnetic selection of transiently transfected cells. *BioTechniques*. 1996;21:876–880. https://doi.org/10.2144/96215st06
22. Ono N, Ono W, Nagasawa T, Kronenberg HM. A subset of chondrogenic cells provides early mesenchymal progenitors in growing bones. *Nat Cell Biol*. 2014;16:1157–1167. https://doi.org/10.1038/ncb3067
23. Oguro H, Ding L, Morrison SJ. SLAM family markers resolve functionally distinct subpopulations of hematopoietic stem cells and multipotent progenitors. *Cell Stem Cell*. 2013;13:102–116. https://doi.org/10.1016/j.stem.2013.05.014
24. Baryawno N, Przybylski D, Kowalczyk MS, et al. A cellular taxonomy of the bone marrow stroma in homeostasis and Leukemia. *Cell*. 2019;177:1915–1932.e16. https://doi.org/10.1016/j.cell.2019.04.040
25. Morrison SJ, Scadden DT. The bone marrow niche for haematopoietic stem cells. *Nature*. 2014;505:327–334. https://doi.org/10.1038/nature12984
26. Campagnoli C, Roberts IA, Kumar S, Bennett PR, Bellantuono I, Fisk NM. Identification of mesenchymal stem/progenitor cells in human first-trimester fetal blood, liver, and bone marrow. *Blood*. 2001;98:2396–2402. https://doi.org/10.1182/blood.V98.8.2396
27. Kuznetsov SA, Friedenstein AJ, Robey PG. Factors required for bone marrow stromal fibroblast colony formation in vitro. *Br J Haematol*. 1997;97:561–570. https://doi.org/10.1046/j.1365-2141.1997.902904.x
28. Dolley-Sonneville PJ, Romeo LE, Melkoumian ZK. Synthetic surface for expansion of human mesenchymal stem cells in xeno-free, chemically defined culture conditions. *PLoS One*. 2013;8:e70263. https://doi.org/10.1371/journal.pone.0070263

29. Nassari S, Duprez D, Fournier-Thibault C. Non-myogenic contribution to muscle development and homeostasis: the role of connective tissues. *Front Cell Dev Biol*. 2017;5:22. https://doi.org/10.3389/fcell.2017.00022
30. Matarraz S, Almeida J, Flores-Montero J, et al. Introduction to the diagnosis and classification of monocytic-lineage leukemias by flow cytometry. *Cytometry B Clin Cytom*. 2017;92:218–227. https://doi.org/10.1002/cyto.b.21219
31. Somaiah C, Kumar A, Mawrie D, et al. Collagen promotes higher adhesion, survival and proliferation of mesenchymal stem cells. *PLoS One*. 2015;10:e0145068. https://doi.org/10.1371/journal.pone.0145068
32. Song JH, Kim JW, Lee MN, et al. Isolation of high purity mouse mesenchymal stem cells through depleting macrophages using liposomal clodronate. *Tissue Eng Regen Med*. 2022;19:565–575. https://doi.org/10.1007/s13770-021-00412-6
33. Siclari VA, Zhu J, Akiyama K, et al. Mesenchymal progenitors residing close to the bone surface are functionally distinct from those in the central bone marrow. *Bone*. 2013;53:575–586. https://doi.org/10.1016/j.bone.2012.12.013
34. Nakamura Y, Arai F, Iwasaki H, et al. Isolation and characterization of endosteal niche cell populations that regulate hematopoietic stem cells. *Blood*. 2010;116:1422–1432. https://doi.org/10.1182/blood-2009-08-239194
35. Schepers K, Pietras EM, Reynaud D, et al. Myeloproliferative neoplasia remodels the endosteal bone marrow niche into a self-reinforcing leukemic niche. *Cell Stem Cell*. 2013;13:285–299. https://doi.org/10.1016/j.stem.2013.06.009
36. Naito AT, Sumida T, Nomura S, et al. Complement C1q activates canonical Wnt signaling and promotes aging-related phenotypes. *Cell*. 2012;149:1298–1313. https://doi.org/10.1016/j.cell.2012.03.047
37. Pajarinen J, Lin T, Gibon E, et al. Mesenchymal stem cell-macrophage crosstalk and bone healing. *Biomaterials* 2019;196:80–89. Special issue: Novel molecular and cellular strategies to optimize bone healing. https://doi.org/10.1016/j.biomaterials.2017.12.025
38. Maggini J, Mirkin G, Bognanni I, et al. Mouse bone marrow-derived mesenchymal stromal cells turn activated macrophages into a regulatory-like profile. *PLoS One*. 2010;5:e9252. https://doi.org/10.1371/journal.pone.0009252
39. Lu D, Xu Y, Liu Q, Zhang Q. Mesenchymal stem cell-macrophage crosstalk and maintenance of inflammatory microenvironment homeostasis. *Front Cell Dev Biol*. 2021;9:681171. https://doi.org/10.3389/fcell.2021.681171

JBMR Plus, 2025, 9, ziaf047
https://doi.org/10.1093/jbmrpl/ziaf047
Methods and Techniques